16th Australasian Fluid Mechanics Conference
Crown Plaza, Gold Coast, Australia
2-7 December 2007

Aerodynamic Effects on an Automotive Rear Side View Mirror

F. Alam, R. Jaitlee and S. Watkins

School of Aerospace, Mechanical and Manufacturing Engineering
RMIT University, Melbourne, VIC 3083, AUSTRALIA

Abstract

The function of a rear view mirror is a determining factor in its shape – resulting in a flat rear mirrored face. The resulting bluff body generates unsteady base pressures which generate unsteady forces, leading to movement of the mirror surface and potential image blurring. Therefore, the objective of this study is to experimentally determine the fluctuating base pressure on a standard and modified mirror using a half of the full-size vehicle, fixed to the side wall of RMIT Industrial Wind Tunnel as well as in isolation (without the half car). A dynamically responsive multi channel pressure system was used to record the pressures. The modification to the mirror consisted of a series of extensions to the mirror rim, to see if this method would attenuate the fluctuating base pressures. The results indicate that increasing the length of the extension changes the pressure pattern across the face, and the over all magnitude of the fluctuations reduces with increasing length of extension.

Introduction

Pressure fluctuations from the wake of the side rear view mirror can lead to vibration of mirror glass, which impairs the driver's vision and consequently, can jeopardize the safety of the vehicle and its occupants. The location and functionality of vehicle side view mirrors is a major contributor to the driver's vision. Although some studies (Milbank et al [2], Oswald [3], Watanabe et al. [4], Watkins [4, 5, 6]) have been undertaken to investigate the structural input (engine, road/tyre interaction etc) as well as aerodynamic input to mirror vibration, very little study was undertaken to quantify the aerodynamic input to mirror vibration. The problem is complex due to the mirror location in the vicinity of the A-pillar vortex. Although the size of the A-pillar vortex is not very large at this location the strength and intensity is very high, Alam [1]. Therefore, the primary objective of this work as a part of a larger study was to measure the aerodynamic pressures (mean and fluctuating) on the mirror surface to understand the aerodynamic effects on mirror vibration. Additionally, the mirror was modified by shrouding around the external periphery (24mm, 34mm, and 44mm extensions) to determine the possibility of minimisation of aerodynamic pressure fluctuations.

Experimental Procedures and Data Acquisition

The mean and fluctuating pressures were measured using a production rear side view mirror fitted to a Ford AU Falcon in the RMIT Industrial Wind Tunnel. The car was cut along its plane of symmetry, thus only replicated the case of zero yaw. The reason for using the car segment as compared to a complete car was to minimise the blockage effect (~15%). Airflow around the mirror was visualized with smoke and documented. The RMIT Industrial Wind tunnel is a closed return circuit wind tunnel with the maximum speed of 150 km/h. The tunnel's working section is rectangular with dimension of 3 m wide, 2 m height and 9 m long. The model (car segment) and test section is shown in Figure 1.

In order to measure the mean (time-averaged) pressures and fluctuating pressures (time-dependent) on the mirror, a Dynamic Pressure Measurement System (DPMS) developed by Turbulent Flow Instrumentation (TFI) was used. Figure 3 shows the various components of the DPMS system. The DPMS is a multi channel pressure measurement system that can accurately measure the fluctuating pressure up to 1000Hz depending upon tubing diameters and lengths. The glass of the mirror was replaced with an Aluminium plate (2.4 mm thickness) and the mirror case was slightly modified in order to hold the aluminium plate and allow exit of the pressure tubing. There were 51 holes made in the aluminium plate in a rectangular grid pattern. The outer diameter and inner diameter of the tubing was 2.4 mm 0.9 mm respectively. The distances between the two adjacent holes were 25 mm horizontally and 13 mm vertically. The silicon rubber tubing was connected to four pressure sensor modules, each having 15 channels. All pressure sensor modules were connected to an interface box that provided power and multiplexed the inputs to the data acquisition system. Figure 2 shows the schematic layout of the pressure measurement of the rear view mirror.

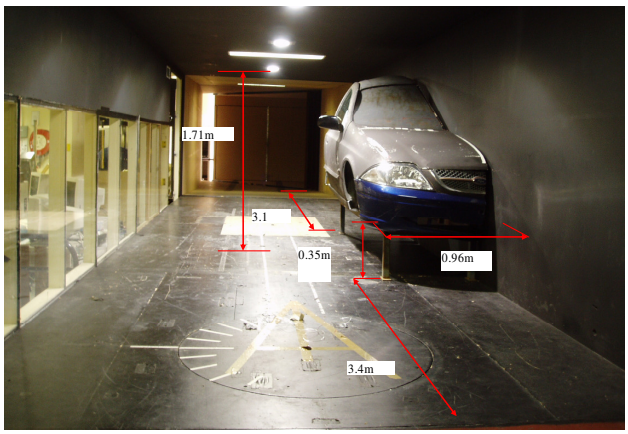

Figure 1: A quarter car with side mirror in the test section of RMIT Industrial Wind Tunnel

The DPMS data acquisition software provided mean, rms (standard deviation), minimum and maximum pressure value of each pressure port on mirror. By entering dimensions (diameter and length) of the tubing used, the data were linearised to correct for tubing response in order to obtain dynamic pressure measurements. The sampling frequency of each channel was 1250 Hz. It may be noted that the peak energy of fluctuating pressure on mirror surface was well below 500 Hz. The mean and fluctuating pressures were measured at a range of speeds (60 to 120 km/h with an increment of 20 km/h) at zero yaw angles. The mirror was tested as standard and then modified by adding 24mm, 34mm and 44mm shrouding on the mirror periphery. The dynamic pressures were converted to fluctuating pressure

coefficient ($C_{p\ rms}$), where $C_{p\ rms} = \frac{p_{std\ dev}}{\frac{1}{2}\rho v^2}$ and ρ is the air density, and v is the free stream air velocity acquired from the tunnel data acquisition system.

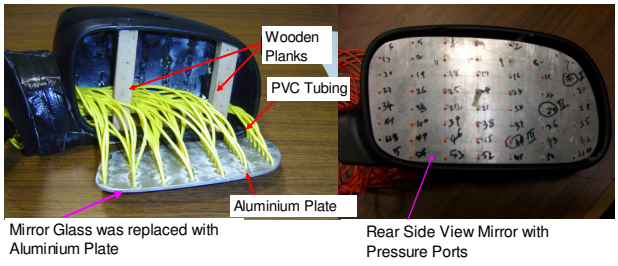

Figure 2: Location of pressure measurement ports with tubing

During the test, the deviation of tunnel air speeds was <1%. Slow fluctuations of tunnel air temperature and ambient pressure were accounted for in the acquisition systems. The estimated error in air density was approximately 1.5%. Using the standard approximations formula, approximate error of 1.5% in *Cp* and *Cp rms* was found, which can be considered within acceptable limits. The turntable aligning errors while yawing the models was less than ±0.2°.

Results and Discussions

Standard Mirror

Three dimensional (3-D) plots of fluctuating pressure coefficients ($C_{p\ rms}$) for the standard mirror are shown in Figures 3 and 4 for the speeds of 60 km/h and 120 km/h. Origin of the plot is located at the top left hand corner position. The x-distance is horizontal and y-distance is vertically down. 2 D contour plots for the standard mirror are shown in Figures 5 and 6 respectively. The plots for other speeds are not shown here due to space constraints. The 3-D plots clearly show that the fluctuating pressure is not uniformly distributed on mirror surface, rather it is concentrated at lower central part of the mirror surface. At low speeds, the maximum fluctuating pressure coefficients were measured at the bottom right part of the mirror surface. However, with an increase of speeds, the magnitude of fluctuating pressure coefficients decreases. The maximum fluctuating pressure shifts towards the bottom central part of the mirror surface.

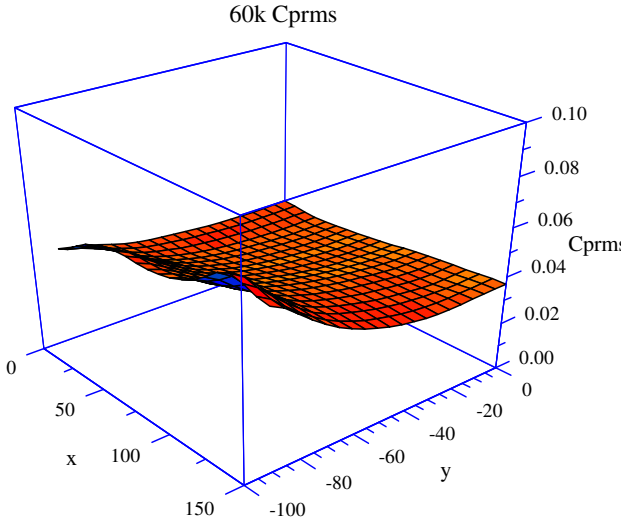

Figure 3: Fluctuating Pressure Coefficients (Cp rms) -3D - 60 km/h

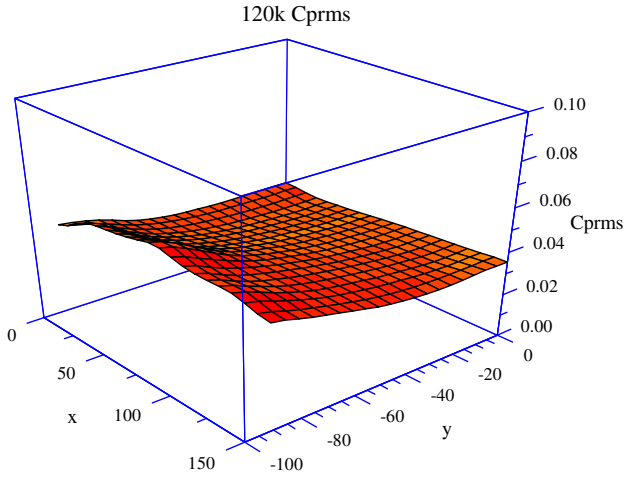

Figure 4: Fluctuating Pressure Coefficients (Cp rms) -3D -120 km/h

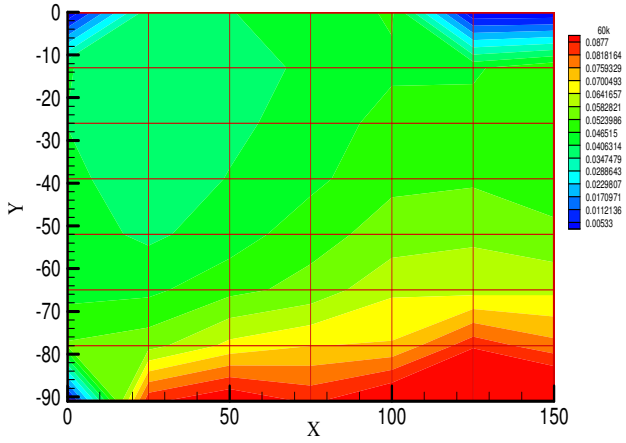

Figure 5: Fluctuating Pressure Coefficients (Cp rms) -2D - 60 km/h

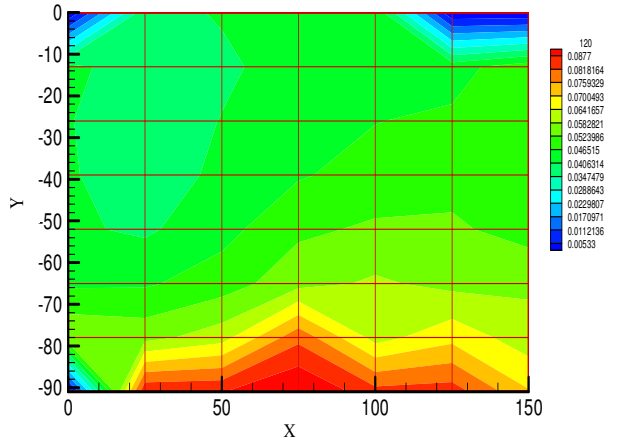

Figure 6: Fluctuating Pressure Coefficients (Cp rms) -2D - 120 km/h

Modified Mirror

As mentioned earlier, the standard mirror was modified with 24 mm, 34 and 44 mm shrouds to see the effects on mirror surface pressure fluctuations. Figure 7 shows the case of the 24 mm shroud length.

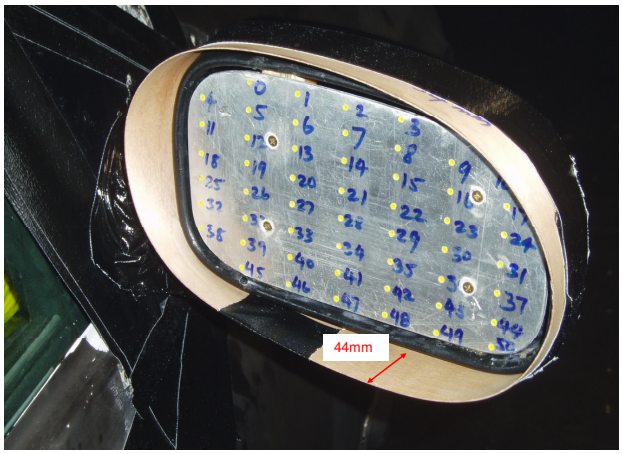

Figure 7: Shrouding of 24mm

The 3-D and contour plots of the fluctuating pressure coefficient for 60 km/h and 120 km/h are shown in Figures 8 & 9 and 10 & 11 respectively. The figures show that the maximum fluctuating pressure coefficient is on the top central part of the mirror, but in case of the 34mm shrouds the magnitude of this fluctuating pressure coefficient has decreased in this area compared with a 24 mm long shroud. Moreover, a drop was also achieved on the bottom central part of the mirror face showing the effects of this shrouding on the mirror face.

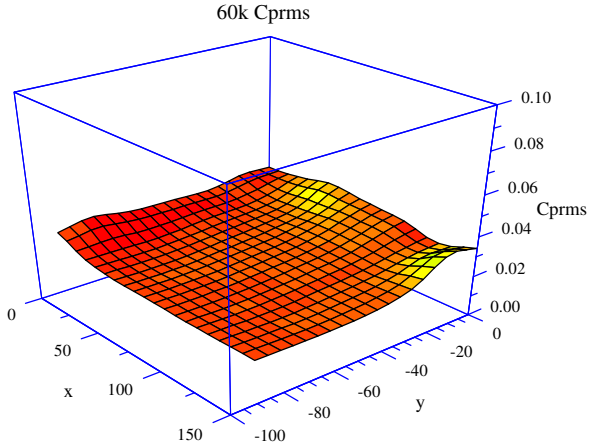

Figure 8: Fluctuating Pressure Coefficients (Cp rms) -3D - 60 km/h

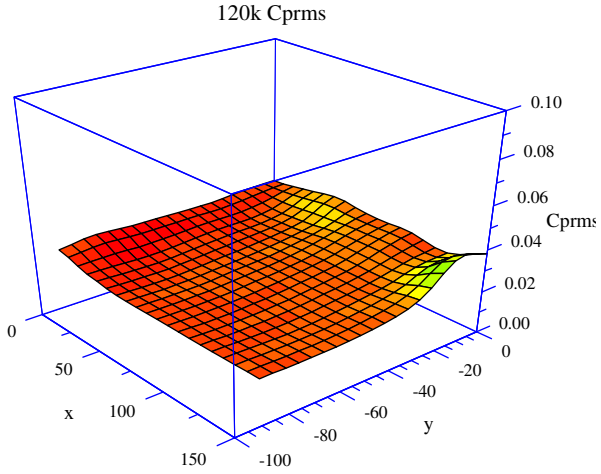

Figure 9: Fluctuating Pressure Coefficients (Cp rms) -3D - 120 km/h

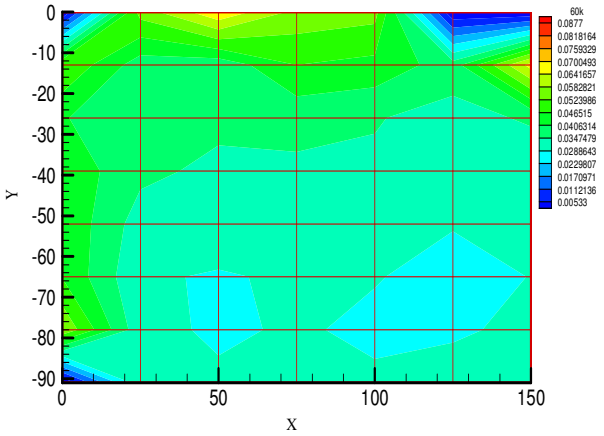

Figure 10: Fluctuating Pressure Coefficients (Cp rms) – 2D -60 km/h

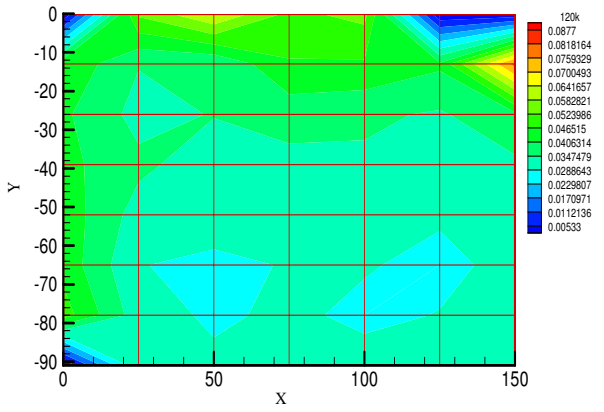

Figure 11: Fluctuating Pressure Coefficients (Cp rms) – 2D -120 km/h

Power Spectral Density (PSD) Analysis

Power spectral density analysis was conducted for the highest fluctuating pressure coefficients for each individual case (both standard and modified mirrors) at all speeds (60 km to 120 km/h with an increment of 20 km/h). In the case of the standard mirror the maximum fluctuating pressure coefficients were observed near to bottom section of the mirror (Pt. 47) as shown in Figure 12. However, this was not the case for the shrouding of 24 mm; 34 mm and 44 mm. The PSD plot for 44 mm shroud is shown in Figures 13 & 14. Plots for other shrouds are not shown here due to space constraints.

There is slight variation in energy distribution for the standard and modified (shrouded) mirror. The spectral density plots generally show that the magnitude of energy distribution reduces with the increase of shrouding length through out the frequency range. However for the 24 mm shroud there is a slightly higher pressure fluctuation at low frequencies. Figures 13 and 14 show the power spectral density for all speeds at point 47. There is a slight decrease in the power spectral density as the shroud length is increased.

It may be noted that all measurements in this study are specific for vehicle, mirror geometry, particularly the A-pillar influence. Although the effects of the mirror position and phase angles were studied, the results were not presented here.

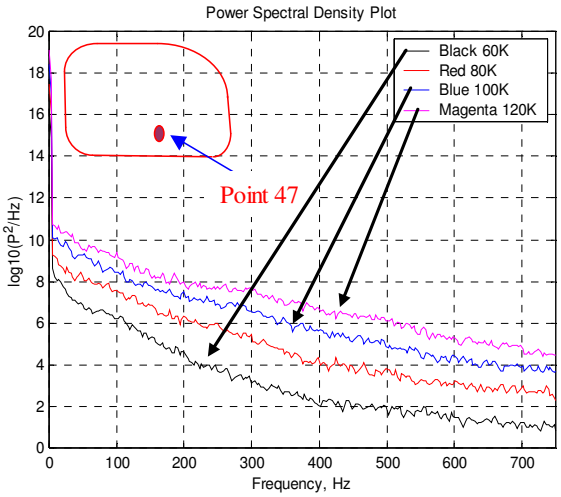

Figure 12: Highest Cp rms at Point 47 for standard mirror

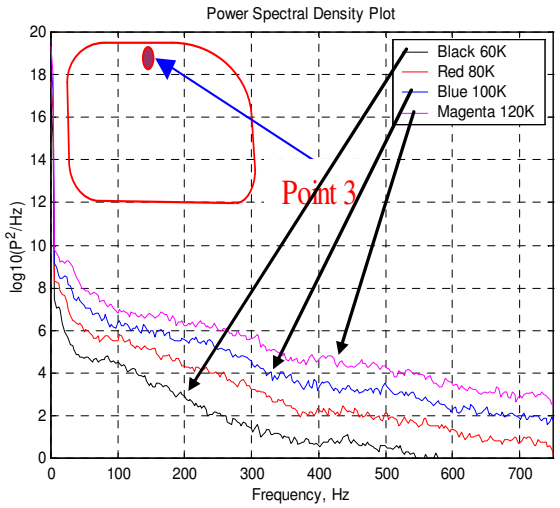

Figure 13: Highest Cp rms at Point 3 for 44 mm shroud mirror

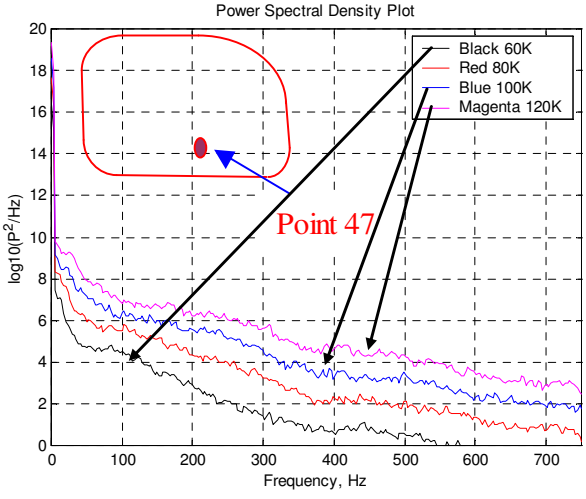

Figure 14: Highest Cp rms at Point 47 for 44 mm shroud mirror

Conclusions

The following conclusions were made from the work presented here (it should be noted that these results are for a specific vehicle and mirror geometries):

- Fluctuating aerodynamic pressures are not uniformly distributed over an automobile mirror surface.
- The highest magnitude of fluctuating pressure for the standard mirror was found at the central bottom section of the mirror surface.
- The highest magnitude of fluctuating pressure was found at the central top section of the mirror surface for all shroud lengths. However, with an increase of shroud length, the magnitude decreases.
- Extending the outer periphery of a typical automotive rear view mirror generally reduces the magnitude of the base pressure fluctuations and changed the distribution across the mirror face.
- Spectral analysis at selected points on the base revealed that most of the energy was concentrated in the lower frequencies- typically less than about 50 Hz. With shrouding present, the distribution changed slightly.
- Further work is recommended, where the phase of the pressure fluctuations need to be understood, in order to clarify the aerodynamic inputs to mirror vibration.
- As the yaw angle is also known to affect mirror noise and vibration, this should also be considered in future work.

Acknowledgments

The authors would like to express their sincere thanks to Ford Motor Company of Australia for proving the test car and Schefenecker Vision Systems for supplying mirrors and CAD models. We are also grateful to Mr Gil Atkins, School of Aerospace, Mechanical and Manufacturing Engineering, RMIT University for his technical assistance with the testing.

References

[1] Alam, F., "*The Effects of Car A-pillar and Windshield Geometry on Local Flow and Noise*", Ph.D. Thesis, Department of Mechanical and Manufacturing Engineering, RMIT University, Melbourne, Australia, 2000.

[2] Milbank, J., Watkins, S. and Kelso, R., "*An Instance of cavity Resonance with an Open-jet free Shear Layer*", Proceedings of the 14th Australasian Fluid Mechanics Conference, 9-14 December, Adelaide, Australia, 2001.

[3] Oswald, G., "*Influence of Aerodynamics on the operating performance of Automotive External Rear View Mirror*", Ph.D. Thesis, Department of Mechanical and Manufacturing Engineering, RMIT University, Melbourne, Australia, 1999.

[4] Watanabe, M., Harita, M., and Hayashi, E., "*The Effect of Body Shapes on Wind Noise*", Society of Automotive Engineering International (SAE) Technical Paper, No.780266, 1978.

[5] Watkins, S., "*On the Causes of Image Blurring in External Rear View Mirrors*", SAE Papers 2004-01-1309, SP- 1874, Detroit, Michigan, USA, 2004.

[6] Watkins, S., Oswald, G. and Czydel, R., *"Aerodynamically-Induced Noise and Vibration of Automobile Add-Ons-External Mirrors, Aerials and Roof racks"*, The 9th International Pacific Conference on Automotive Engineers, Bali, Indonesia, 1997.

[7] Jaitlee, R., Alam, F. and Watkins, S., *"Pressure Fluctuations on Automotive Rear View Mirrors"*, SAE World Congress, SAE 2007-01-0899 in Vehicle Aerodynamics 2007, SP-2066, ISBN 978-0-7680-1856-1, 16-19 April, Detroit, Michigan, USA, 2007.